

Improving the Exploration of Deep Reinforcement Learning in Continuous Domains using Planning for Policy Search

Jakob J. Hollenstein, Erwan Renaudo, Matteo Saveriano, Justus Piater

¹Department of Computer Science, University of Innsbruck, Innsbruck, Austria
{name.surname}@uibk.ac.at

Abstract

Local policy search is performed by most Deep Reinforcement Learning (D-RL) methods, which increases the risk of getting trapped in a local minimum. Furthermore, the availability of a simulation model is not fully exploited in D-RL even in simulation-based training, which potentially decreases efficiency. To better exploit simulation models in policy search, we propose to integrate a kinodynamic planner in the exploration strategy and to learn a control policy in an offline fashion from the generated environment interactions. We call the resulting model-based reinforcement learning method PPS (Planning for Policy Search). We compare PPS with state-of-the-art D-RL methods in typical RL settings including underactuated systems. The comparison shows that PPS, guided by the kinodynamic planner, collects data from a wider region of the state space. This generates training data that helps PPS discover better policies.

1 Introduction

Robots in human-centric environments are confronted with less structured, more varied, and more quickly changing situations than in typical automated manufacturing environments. Research in autonomous robots addresses these challenges using trial-and-error based learning methods. However, learning by trying out actions directly on a real robot is time-consuming and potentially dangerous for the environment and the robot itself. In contrast, physically-based simulation provides the benefit of faster, cheaper, and safer ways for robot learning.

In this context, Deep-Reinforcement Learning (D-RL) has shown promising results (OpenAI et al. 2018), but the training with D-RL algorithms can be tedious and it is often resource demanding. One problem in D-RL training is that most algorithms are gradient-based and thus susceptible to local optima. This is usually countered by adding stochasticity to the action selection (Lillicrap et al. 2016; Haarnoja et al. 2019; Plappert et al. 2017). Although it is known that gradient-based algorithms suffer from the local minima problem, only some papers (Plappert et al. 2017; Henderson et al. 2018) mention it, while the practical implications of the local minima problem are not exhaustively investigated in the D-RL literature.

We believe that insufficient exploration plays a major role in the problem of learning sub-optimal policies. To remedy

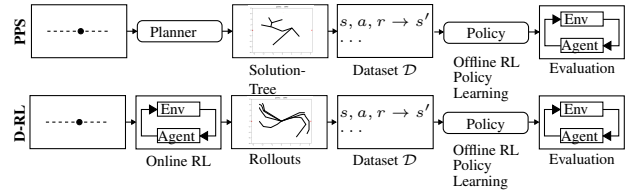


Figure 1: A comparison between PPS and other D-RL methods. In PPS (top) a kinodynamic planner generates interactions— (s, a, r, s') tuples—that are used for offline policy search. In the typical D-RL setting (bottom) the agent directly learns a policy by performing exploratory actions to generate interactions.

this problem, one might increase the search time while keeping the exploration noise high, or, as in this work, use more principled exploration. In the limit increasing search time and exploring using randomly sampled actions, would also yield acceptable solutions. However, exploring by choosing actions to maximize exploration (*directed exploration*) appears more promising to find good solutions more reliably and in less time. We focus on the latter approach and build our method around two key considerations, namely that *i*) covering a *more diverse area* of the state space increases the chances of finding an optimal solution, and that *ii*) moving towards a directed exploration that exploits local dynamics reduces the number of samples required to learn a good policy.

Aiming for diverse and directed exploration and considering that physically-based simulators are typically available for robotic systems, we propose to exploit model-based and physically consistent kinodynamic planners to generate environment interactions, thereby *guiding* the robot exploration, while tackling the problem of planning time by synthesizing the planning results into a policy. We select Rapidly Exploring Random Tree (RRT) (Lavalle 1998) for kinodynamic planning (Glassman and Tedrake 2010; Perez et al. 2012), since this class of model-based planning methods focuses on maximizing state-space exploration (coverage). The data collected via RRT-guided exploration can then be used to learn a policy using an off-policy search method. For policy search, the popular Soft Actor-Critic (SAC) approach (Haarnoja et al. 2019) has been used. The

way we used the robot model for the exploration makes the proposed *Planning for Policy Search (PPS)* approach a model-based reinforcement learning method (Sutton and Barto 2018). In this work, we present the PPS algorithm that combines planning and policy search (see Figure 1) and compare the performance of PPS against the state-of-the-art D-RL approaches Deep Deterministic Policy Gradient (DDPG) (Lillicrap et al. 2016) and SAC (Haarnoja et al. 2019). The aim of this comparison is to answer the following research questions:

- Q1 How do the data generated by PPS compare to those from other D-RL methods – do they cover a larger area of the state space?
- Q2 Are PPS methods less susceptible to local optima than other D-RL methods?

Section 2 presents an overview of the related work. The PPS approach is presented in Sec. 3. The experimental evaluation and the comparison with existing approaches are carried out in Sec. 4. Section 6 discusses obtained results, states the conclusions, and proposes further extensions.

2 Related Work

Using physically-based simulations for learning is limited by the necessity to approximate physical phenomena, causing discrepancies between simulated and real-world results. This difference is called the reality gap and it is a well-known problem in various fields of robotics. For training in simulation and applying in the real world (Sim2Real), filling this gap is crucial. One important method for bridging this gap is Domain randomization (Tobin et al. 2017; Sadeghi and Levine 2017; James, Davison, and Johns 2017): instead of one simulated environment, learning is done using a distribution of models with varying properties such as mass, friction, and force/torque noise. The idea is to make the behavior policies learned by the reinforcement learning process more robust to the differences within this distribution, thereby increasing robustness against the difference between the training distribution and the target domain, i.e. against the reality gap. The work from OpenAI (OpenAI et al. 2018) has shown a successful use of domain randomization for learning in-hand-manipulation; however, the number of required training steps is raised by a factor of 33 when domain randomizations are introduced. This increases the number of training steps to the magnitude of about $3.9 \cdot 10^{10}$ from a magnitude of $1.2 \cdot 10^9$, while classical deep reinforcement learning approaches typically require 10^5 to 10^9 iterations of simulation steps. Many algorithms are tested on 10^6 timesteps, depending on the environment. The required amount of training data can make this method prohibitively expensive, and typically the availability of a simulation model is not exploited.

Improving the efficiency of domain randomization is an active topic of research. Possible ways to increase sample efficiency include using adversarial randomizations (Mandlekar et al. 2017), limiting the training to stop before overfitting to idiosyncrasies of the simulation (Muratore et al. 2018), or using model-based approaches for reinforcement

learning (Chatzilygeroudis et al. 2020; Saveriano et al. 2017; Levine and Koltun 2013). In the context of D-RL, the Guided Policy Search (GPS) (Levine and Koltun 2013) represents a prominent model-based approach. In GPS, roll-outs from a deep neural network controller are optimised by an optimal control method such as the iterative Linear Quadratic Regulator (iLQR) (Todorov and Weiwei Li 2005; Tassa, Erez, and Todorov 2012) method. However, GPS is usually initialized from demonstrations since the exploration capabilities of the underlying optimization method (iLQR) are limited. Furthermore, the optimization method requires a specifically-tailored cost function to guide the search procedure towards relevant solutions.

The benefits arising from combining a model-based method with model-free reinforcement learning were highlighted by Renaudo et al. (2014). However, their work focuses on discrete problems and their model-based and model-free algorithms control the agent jointly, whereas we address continuous RL problems where the planning method produces data for the policy learner.

In this work, we identify *insufficient exploration* as a major cause of convergence towards *suboptimal policies*, which results in an increased training time to find a good policy. Therefore, we propose a more principled exploration method guided by a kinodynamic planner.

Linear Quadratic Regulator (LQR)-RRT (Perez et al. 2012) and Affine Quadratic Regulator (AQR)-RRT (Glassman and Tedrake 2010) are examples of RRT methods that use a dynamics-based cost metric to guide the tree extension, enabling them to deal with kinodynamic planning problems.

While RRT methods are powerful asymptotically complete methods, their computational cost is high, which only allows the plan to be computed offline. Hence, RRT plans are not suitable to be directly used as a control policy for continuous systems. The problem of performance is also recognized in planning, and work is being undertaken to make RRT faster, for example by Wolfslag et al. (2018).

A possible alternative to RRT could be Monte-Carlo Tree Search (MCTS), which is part of the successful AlphaGo (Silver et al. 2016) system. However, vanilla MCTS is not directly applicable to continuous action domains. A second advantage of RRT over MCTS is that, by using local steering functions, they already utilize the locally linearized dynamics often available in continuous systems which can make the search more efficient. In PPS, the planner is used to explore the state space and to collect training data from which a policy is learned. Hence, we do not need to plan at run time when the robot executes the learning policy. We exploit RRT in the training phase as a reasonably powerful, yet reasonably simple kinodynamic planner, although more complex kinodynamic planners can also be used provided they collect environment interactions. In preliminary studies on the 1D Double Integrator benchmark domain (see Table 2) we found indications of increased exploration (Hollenstein and Piater 2019) in the data generated using LQR-RRT as a kinodynamic planner compared to popular D-RL methods. We could already show that better exploration of LQR-RRT generated data improved the performance of policies learned from that data (Hollenstein, Renaudo, and Piater

2019; Hollenstein et al. 2020). In this work we extend on these results by moving from linearized to affine-linearized dynamics, in both the distance metric, thus replacing LQR-RRT with the AQR-RRT, as well as the Model-Predictive-Control (MPC) steering, and most importantly by applying the method to benchmark domains with non-linear dynamics.

3 Planning for Policy Search (PPS)

The key idea of PPS is to exploit kinodynamic planning to guide the reinforcement learning exploration and collect interaction samples $\{s, a, r, s'\}$ where s and s' represent the current and next state respectively, a is the performed action, and r is the obtained reward. The samples collected across different runs are stored in a replay buffer \mathcal{D} and are used to search for an optimal policy using any off-policy search approach in an *offline*- or *batch*-reinforcement learning fashion (Ernst, Geurts, and Wehenkel 2005; Lange, Gabel, and Riedmiller 2012). The proposed PPS approach is summarized in Algorithm 1. We further use x to denote hypothetical states used by the kinodynamic planner which may or may not be feasible states of the environment, v denotes states stored as nodes in the internal tree of the kinodynamic planner, and d denotes trajectories. We also use affine versions of all states v^a, s^a, x^a , which are all related to the non-affine variants in the same way: $x^a = [x^T \ 1]^T$. Note that for readability we will not explicitly include the conversions, but instead assume both variants are available.

3.1 Kinodynamic planning for interaction data collection

We base PPS exploration on a variant of the Rapidly Exploring Random Tree (RRT) that exploits locally affine dynamics and solves an Affine Quadratic Regulator (AQR) problem (Glassman and Tedrake 2010). We refer to this method as AQR-RRT in the rest of the paper. During the exploration phase, the data are collected by iteratively calling the AQR-RRT to extend the tree \mathcal{T} (EXTENDTREE(\mathcal{T}, x_r) in Algorithm 1).

An RRT method consists of three components: *a*) a sampling method that decides where tree extensions should be directed to, *b*) a distance metric that estimates the cost of going from nodes in the tree to a new target state, and *c*) a local steering method, to reach from a given state to a target state.

In the current implementation of PPS, we start from an empty tree \mathcal{T} and add the initial robot state as the root node v_0 . Then, we loop N times to incrementally extend the tree. At each iteration, we uniformly sample the state space to create a new candidate goal state x_r . The minimum distance from each node v_i in the tree to the new state x_r is calculated using the AQR metric. The metric uses $\dot{x} = Ax + Ba + c$ as its model, linearized around x_r . The affine term c is incorporated into the affine matrices $A^a = \begin{bmatrix} A & c \\ 0 & 1 \end{bmatrix}$ and

$B^a = [B^T \ 0]^T$, which are used together with the affine state variants (x^a, s^a, v^a) .

Algorithm 1 Planning for Policy Search (PPS)

```

function PPS
   $\mathcal{T} \leftarrow \{v_0\}$  ▷ Initial State
   $\mathcal{D} \leftarrow \{\}$  ▷ Empty replay buffer
  for  $i \in \{1, \dots, N\}$  do
     $x_r \leftarrow$  random state
     $v_{\text{new}}, d_{\text{new}} \leftarrow$  EXTENDTREE( $\mathcal{T}, x_r$ ) ▷ See Alg. 2
     $\mathcal{T} \leftarrow \mathcal{T} \cup \{v_{\text{new}}\}$  ▷ Add node to tree
     $\mathcal{D} \leftarrow \mathcal{D} \cup d_{\text{new}}$  ▷ Add trajectory to  $\mathcal{D}$ 
  end for
  for  $i \in \{1, \dots, M\}$  do ▷ Perform  $M$  training steps
     $\pi \leftarrow$  OFFPOLICYSEARCH( $\mathcal{D}$ ) ▷ See SAC
  end for
  return  $\pi$  ▷ Found policy
end function

```

Algorithm 2 Extend Tree with AQR-RRT

```

function EXTENDTREE( $\mathcal{T}, x_r$ )
   $h \leftarrow$  user defined horizon
   $v \leftarrow$  AQRNEAREST( $\mathcal{T}, x_r$ )
   $A^a, B^a \leftarrow$  ENV.DYNAMICS( $x_r$ )
   $G^a, H^a \leftarrow$  DISCRETIZE( $A^a, B^a$ )
   $s_{\text{new}}, d_{\text{new}} \leftarrow$  STEER( $v, x_r, h, G^a, H^a$ ) ▷ See Alg. 4
  where
     $d_{\text{new}} = (s_0, r_0, a_0, s_1), \dots, (s_{n-1}, r_{n-1}, a_{n-1}, s_n)$ 
     $s_{\text{new}} = s_n$ 
   $v_{\text{new}} \leftarrow$  STOREPOINT( $s_{\text{new}}, d_{\text{new}}, v$ )
  return  $v_{\text{new}}, d_{\text{new}}$ 
end function

```

The bias term c , which is typically neglected in the standard linearization, accounts for nonzero velocities at the goal (Glassman and Tedrake 2010). This is important since after extending the tree towards x_r , the reached state will be used as the starting point for additional branches of the tree, and reaching and staying (zero velocity) at x_r would be counterproductive. The complete calculation of the AQR metric is given in the Appendix. The AQR distance to x_r , computed for each node in the tree \mathcal{T} , is then used to determine the node $v \in \mathcal{T}$ closest to x_r . This procedure to determine v is referred to as AQR_{Nearest}(\mathcal{T}, x_r) in Algorithm 2.

In the steering method, discrete-time linearized dynamics G^a, H^a are used, which are derived from the continuous-time linearized dynamics A^a, B^a . The node v becomes a starting point, and a steering function (STEER(v, x_r, h, G^a, H^a) in Algorithm 2) is applied to compute a feasible state trajectory that connects v with x_r .

We solve the steering problem using a linear MPC method (Camacho and Alba 2007). In the standard implementation, MPC works by repeatedly solving a quadratic program (QP) from the current state $x_0 \leftarrow v$ to the goal x_r over a finite time horizon h . The solution of the QP program is a trajectory of control inputs $a_k, k = 0, \dots, h - 1$ that drives the robot from x_0 to x_r within h steps. The first control a_0 is then used to command the robot to attain a new state s_1 . This procedure (solving the QP and making one controlled step) is repeated, where x_0 is replaced $x_0 \leftarrow s_1$. Starting

from this new state x_0 the QP is solved and another action a_0 is taken. The system thus converges to the state x_r and stays there.

In our implementation, we adopt a slightly modified version of the linear MPC that makes use of a shrinking (in contrast to the receding) horizon to let the robot reach the goal position with nonzero velocity. While we also start solving the QP with a horizon $h_0 \leftarrow h$ and take step a_0 , in the next repetition, the horizon h_i is shortened by one step $h_{i+1} \leftarrow h_i - 1$. Thus we will reach x_r after a total of h steps. If we did not shorten the horizon and let the search run for m steps, then we would expect to reach the goal state x_r at state x_{h-m} of the current predicted horizon; however, after this point m more steps (x_{h-m}, \dots, x_m) will be taken. Minimizing the cost associated with these remaining steps drives the system away from x_r if the velocity at x_r is nonzero, and thus motivates shortening the horizon. In some cases, the environment’s constraints might not allow for exactly reaching x_r and the optimization might become infeasible and fail. In these cases, the state actually reached by the steering procedure will be returned. The complete steering method is given in the Appendix. The result of the steering procedure is a new node v_{new} that is added to the tree \mathcal{T} and a trajectory d_{new} of intermediate states, actions, and rewards that are added to the replay buffer \mathcal{D} .

3.2 Transform interaction data into a control policy

As stated previously, the procedure used by RRT to grow the tree (see Algorithm 2) is computationally expensive and becomes rapidly incompatible with real-time control requirements. Learning a policy solves this issue since no planning step is needed during the execution. Importantly, we use the original RRT and not the RRT* (Karaman and Frazzoli 2011) variant. The difference between RRT and RRT* is that the latter iteratively reconnects and improves paths and thus converges to shortest paths, which RRT is not guaranteed to do. However, this comes at a price: to reconnect nodes with shorter paths, the steering function has to be used, which performs environment steps. Thus the use of RRT* would incur additional interactions on the simulated environment to perform this optimization. Since we first want to find areas close to the rewards and then, in the future, perform local finetuning using the D-RL method directly, it does not make sense to spend environment steps on improving all paths.

After the completion of the data collection, \mathcal{D} consists of a set of simulated (environment) interactions that can be used to search for an optimal control policy using an off-policy search method. We collect the data by maximizing the coverage of the state space, rather than searching for high-reward regions.

In PPS therefore \mathcal{D} constitutes a fixed replay buffer and is used to train a policy (OFFPOLICYSEARCH(\mathcal{D})) in Algorithm 1) without generating new environment data during the policy search. The learned policy is then evaluated on the environment. In this work we use SAC (Haarnoja et al. 2019) as the off-policy learning method. It uses a stochastic policy and an actor-critic approach. It explores by sampling actions from the stochastic policy, and adds an entropy term

to the value-function loss to encourage more exploratory behaviour of the policy; that is, high entropy in the action selection is encouraged.

4 Experimental Evaluation

Reinforcement learning agents collect experience and use that experience to learn a policy, either implicitly in on-policy algorithms such as Proximal Policy Optimization (PPO) (Schulman et al. 2017) or Trust-Region Policy Optimization (TRPO) (Schulman et al. 2015), or explicitly in algorithms such as DDPG or SAC which use a replay buffer. Thus, the exploration process should reach regions in the state space relevant for the task so that it can learn a well-performing policy. If it cannot reach high-reward areas of the state space, the learned policy will also not move the agent to these regions and therefore the achieved return will be lower.

We assume that exploration and performance are linked and test whether using the PPS method increases exploration (Q1). We measure exploration by area of covered state space.

Since this is only a necessary but not a sufficient property, we also test whether these data allow us, on average, to learn more successful policies, and thus are less susceptible to local optima (Q2). We measure this by learning policies from the collected data and evaluating the returns of these policies.

We compare the performance to the popular off-policy D-RL algorithms DDPG (Lillicrap et al. 2016) and SAC (see Section 3.2).

DDPG is an off-policy method that learns a deterministic policy using an actor-critic approach. Exploration is done by using the deterministic policy and adding exploration noise to the selected actions.

We use the implementations provided by Hill et al. (2018) which are a tuned and improved version of the algorithms provided by Dhariwal et al. (2017). We exclude the hyperparameters from the policy search and assume that the algorithms are robust over a wide range of environments using the default values of the hyperparameters.

4.1 Q1 – Comparing data generation

To compare the exploration, we collect the data the agents see during their learning phase (see Figure 1). These data are then analysed for state-space coverage. The coverage is calculated as the percentage of nonempty bins. For simplicity we use uniformly-shaped bins. The number of bins is equal along each state-space dimension and is set to $\text{divisions} = \left\lceil \left(\frac{N}{5}\right)^{\frac{1}{d}} \right\rceil$, i.e. such that, in the uniform case, we expect five data points in each bin on average. Because of the ceiling operator, the total number of bins $n_{\text{bins}}^d = \text{divisions}^d$ can exceed N . This is especially true in high dimensional cases, where this will lead to many more bins than there are datapoints. To compensate for this, we scale the resulting number of nonempty bins by $\max \left\{ \frac{n_{\text{bins}}^d}{N}, 1 \right\}$

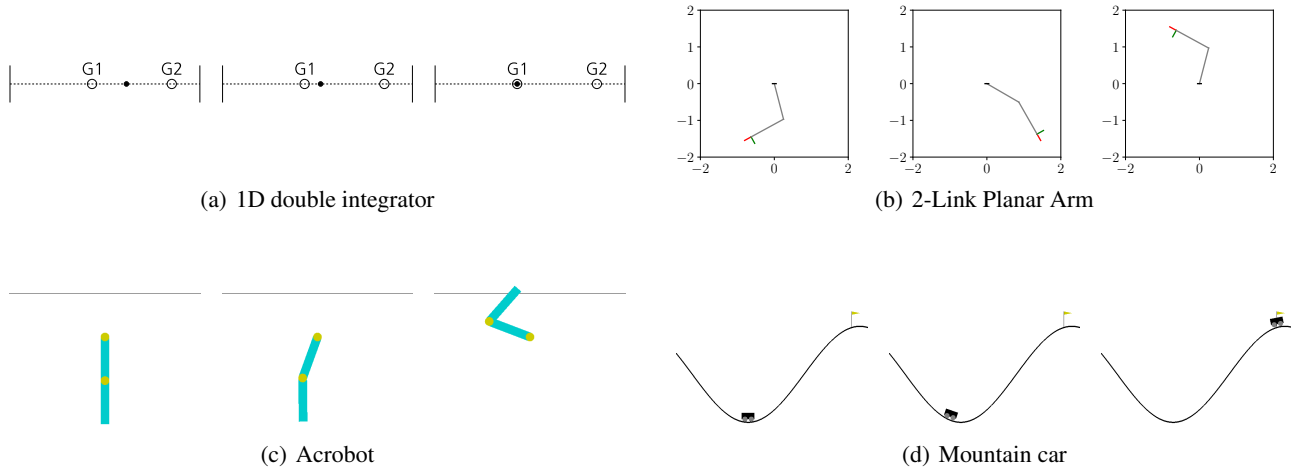


Figure 2: Environments used for testing. For each environment, the different snapshots show the initial, an intermediate, and the final condition.

4.2 Q2 – Susceptibility to local optima

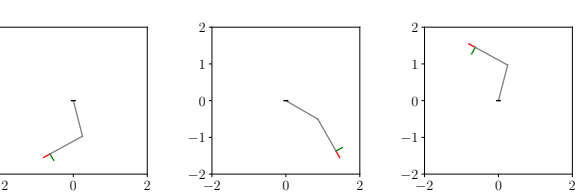
We perform training runs with DDPG, SAC and our PPS method. After the agents have learned, we use their policies to generate evaluation returns, which we analyze to compare their performance. This is done on 10 independent learning runs.

While the DDPG and SAC agents learn directly on the environment, our PPS agent uses the planner (AQR-RRT) to generate data. The generated data are stored in a replay buffer. The replay buffer is fixed – no experience is added, no experience is removed and an off-policy algorithm (SAC) is used to learn from this buffer. As a baseline this experiment is also performed for data generated by an SAC agent and by a DDPG agent. The data of both are also used in fixed SAC replay buffers to learn policies. We fixed the SAC entropy coefficient hyperparameter to 0.1^1 instead of automatically adjusting it, since we noticed instability when learning from a fixed buffer. To allow the same entropy coefficient across different environments (reward ranges), we normalized the rewards in \mathcal{D} to have zero mean and unit standard deviation.

We compare the performance on four environments that are depicted in Figure 2. In all four environments the agent starts in the same state configuration and has to reach a goal region.

1D Double Integrator is a force-controlled, one-dimensional point mass in a position-wrap-around environment. The state space consists of position and velocity. The environment features two goal locations. The agent starts closer to a lower-reward goal region and has to move away from this region in order to reach the second, higher-reward goal location. For further details see Table 2 in the appendix.

2-Link Planar Arm is a torque-controlled, 2-link planar arm implemented following the description by Žljajpah



(b) 2-Link Planar Arm



(c) Acrobot



(d) Mountain car

(1998). While the arm is torque controlled and the state space consists of joint positions and joint velocities, the reward is given in the task space. The direct path is blocked due to joint limits. The feasible path involves moving away from the task-space goal, incurring less reward, but ultimately achieving maximum returns.

Acrobot is the Acrobot (Murray, Murray, and Hauser 1990) from OpenAI Gym (Brockman et al. 2016). We modified the agent to use continuous actions $a \in [-1, 1]$ and changed the state representation to angle and angular velocity. In our version, the agent always starts in the lowest-energy position.

Mountain Car is the continuous mountain car (Moore 1990) from Brockman et al. (2016). Here we modified the starting position to be the lowest-energy state, which makes the environment harder, as it is less likely to be solved by chance.

For the latter three environments we used JAX (Bradbury et al. 2018) to derive the linearized dynamics and speed up computations.

5 Results

5.1 Q1 – Comparing data generation

The exploration as measured by the proportion of state space covered is shown in Table 1. The median coverage of ten independent runs as well as the interquartile range (IQR; in parentheses) after 10^5 interaction steps are listed. In all four environments PPS achieves the highest state-space coverage, with a margin significantly larger than the IQR in all cases but the Mountain Car. DDPG appears to be exploring more than SAC in most cases, except when exploration is very low (Acrobot), where both SAC & DDPG explore very little.

¹We tested entropy coefficients in the range of $0.005 \dots 10$.

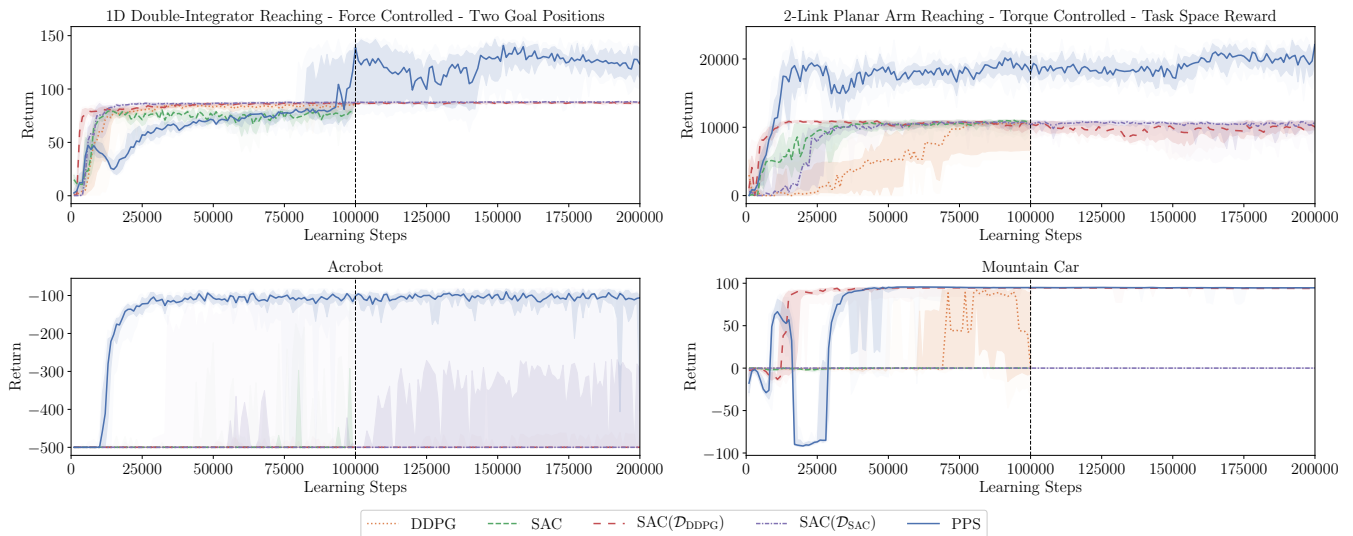


Figure 3: Learning curves obtained with DDPG, SAC, and PPS (ours). The graphs show returns achieved by evaluation roll-outs in the respective environment after training the policy for the given number of learning steps. The indirect methods ($SAC(\mathcal{D}_{DDPG})$, $SAC(\mathcal{D}_{SAC})$) and PPS are trained on a fixed replay buffer \mathcal{D} , filled with 10^5 environment interactions (the $2 \cdot 10^5$ learning steps do not add any further interactions to \mathcal{D}). DDPG and SAC, which directly learn as they collect environment interactions, are also shown for 10^5 steps (and thus stop at the vertical center line). These 10^5 collected environment interactions are used to train $SAC(\mathcal{D}_{DDPG})$ and $SAC(\mathcal{D}_{SAC})$.

| Environment | DDPG | SAC | PPS |
|----------------------|--------------------------|--------------------------|---------------------------------|
| 1D Double Integrator | 22.5% ($\pm 2.4\%$) | 18.9% ($\pm 4.8\%$) | 93.7% ($\pm 1.0\%$) |
| 2-Link Planar Arm | 32.1% ($\pm 3.0\%$) | 9.3% ($\pm 2.0\%$) | 84.6% ($\pm 0.5\%$) |
| Acrobot | 0.1% ($\pm 0.5\%$) | 1.8% ($\pm 3.4\%$) | 15.0% ($\pm 0.3\%$) |
| Mountain Car | 52.5% ($\pm 8.9\%$) | 16.1% ($\pm 3.9\%$) | 54.4% ($\pm 1.5\%$) |

Table 1: State-space coverage as visited percentage of bins. Each number represents the median of ten independent runs, the interquartile range is listed in brackets.

5.2 Q2 – Susceptibility to local optima

Figure 3 depicts the evaluation returns during learning for the baselines (DDPG, SAC), as well as PPS. In each environment ten independent runs are performed. The median evaluation return is depicted, with the shaded area showing the IQR around the median. We use tanh activations in the indirectly-trained policies (and PPS) because we found them to produce results with smaller variance and to perform more robustly when learning from the fixed buffer.

While the collection phase consists of 10^5 steps, the plots depict learning curves for $2 \cdot 10^5$ steps. In the indirect cases, the replay buffer is fixed so the x -axis steps only correspond to learning steps, not to environment interaction steps – which are mixed (collecting & learning) in the case of the

direct algorithms SAC and DDPG.

The results show improved performance when training on the fixed replay buffer. They also show performance of PPS to be superior to the policy indirectly trained on SAC data as well as the directly-trained SAC policy. However, from the learning curves, it appears the variance is higher in the PPS learning process, and in some cases (Mountain Car, Double Integrator) dips after initially rising, before reaching high performance. On the Acrobot PPS performs a lot better than the other algorithms. The Acrobot is a hard problem because it is underactuated and taking the wrong actions will push the agent back to a state that is further away from the goal. Moreover, the reward is very sparse, with zero reward except for reaching the goal region. Here, the directed exploration of PPS is able to unleash its full potential.

In the Mountain Car environment, PPS reaches a similar performance to training SAC from DDPG data, while the policies trained by DDPG exhibit high variance in their returns and SAC achieves zero returns. This striking result of SAC presumably stems from the reward structure in the Mountain Car environment, where a large positive reward is attributed when the goal is reached, while each action is penalized according to its effort. Here, SAC optimizes for the closest local minimum: not taking any actions. In the cases of the Double Integrator and the Planar Arm, both DDPG and SAC pick up on the shaped reward and optimize towards the local minimum, while PPS, although with less data density and thus higher variance, reaches the high-reward areas. Surprisingly in many cases, it appears that SAC is more successful when learning from DDPG data than when learning from SAC data itself.

6 Discussion

In this work, we investigated whether directed exploration in PPS reduces the probability of getting stuck in a local optimum compared to undirectedly exploring gradient based D-RL methods. Our experiments show that this can indeed be a problem in practice, even in relatively small toy problems such as the double integrator with two local optima. On average the agent controlled by PPS explores a wider part of the state space than D-RL methods that focus on reward accumulation. While this is partly expected due to the exploration/exploitation tradeoff, our experiments show that even from this highly-exploratory data good policies can be learned and can even surpass the performance of the agents focusing more on exploitation. This shows that by using directed exploration PPS reduces the probability of getting stuck in local optima compared to undirectedly exploring D-RL methods.

The data gathered by PPS are not biased by reward accumulation and are thus more representative of the environment. This should make these data quite suitable for reuse in different tasks. This is also visible in Table 1 where the coverage is reduced for the underactuated and thus harder-to-control environments (Acrobot, Mountain Car) where the coverage is impacted by the difficulty of the environment dynamics. Also in these cases the coverage achieved by PPS dominates that of the baseline algorithms.

Although PPS is able to achieve better policies than the other methods, it also exhibits more variance in the learning process. Presumably this stems from the extreme off-policy nature of our algorithm which should increase the variance in the gradient estimates. This instability during continued learning on the fixed buffer (timesteps beyond 10^5 in Figure 3) is also present when learning from data collected by the D-RL methods and warrants future research.

One limitation of our study is that the evaluations are done on relatively low-dimensional tasks. Uniformly covering the state space might reach its limitations in high-dimensional problems due to the curse of dimensionality: A goal or high-reward region might be too narrow to be covered by uniformly-distributed samples. However, this problem can be alleviated by changing the uniform sampling mechanism to a reward-adaptive procedure which we will investigate in future work. We envision our method to be most useful in scenarios where a model is already available (for example model-based RL with an already-learned model to adapt to a different task) or even more importantly in the regime of Sim2Real training where a simulation model is used to train robust policies that can then be applied to the real system. In recent years the approach of domain randomization has gained attention where properties of the simulation model are randomized thereby forcing the policy to be robust to model inaccuracies and preventing overfitting to idiosyncrasies of the simulation. In this setting our method has the potential to speed up domain-randomized training: By randomizing the model, using planning to quickly discover potential new goal regions and adapting the sampling to re-use prior knowledge of similar tasks, the method can potentially focus the training on relevant parts of the state space and reduce the number of necessary samples. This will be evaluated in

Algorithm 3 Calculate AQR & find nearest neighbor

```

function AQRDISTANCE( $x_0, x_r$ )
  Let  $A, B, c$   $\triangleright$  linearized dynamics around  $x_r, x_0$ 
   $\bar{x}_0 = x_0 - x_r$ 
   $\dot{P}(t) = AP(t) + P(t)A^T - BR^{-1}B^T$ ,
   $P(T) = 0, t \in \{T, \dots, 0\}$ 
   $S^{-1}(t) = P(t)$ 
   $d(\bar{x}_0, T) = e^{AT}\bar{x}_0 + \int_0^T e^{A(T-\tau)}c d\tau$ 
   $J^*(\bar{x}, T) = T + \frac{1}{2}d^T(\bar{x}_0, T)S^{-1}(T)d(\bar{x}_0, T)$ 
   $T^* = \arg \min_T J^*(\bar{x}_0, T), 0 \leq T \leq T_{max}$ 
  return  $J^*(\bar{x}_0, T^*), T^*$ 
end function
function AQRNEAREST( $\mathcal{T}, x_r$ )
  return  $\arg \min_{v \in \mathcal{T}} \text{AQR}_{\text{DISTANCE}}(x_v, x_r)$ 
end function

```

Algorithm 4 Local steering model-predictive control method.

```

function STEER( $v, x_r, h, G^a, H^a$ )
   $d \leftarrow ()$   $\triangleright$  empty trajectory
   $s \leftarrow v$   $\triangleright$  initialize state
   $x_r \xleftarrow{a} x_r$ 
  for  $L \in \{h, \dots, 1\}$  do  $\triangleright$  Shrinking Horizon
     $x_0 \xleftarrow{a} s$   $\triangleright$  all  $x$  are affined
    With  $Q_L \gg Q$ 
    minimize  $(x_L - x_r)^T Q_L (x_L - x_r) +$ 
       $\sum_{k=0}^{L-1} (x_k - x_r)^T Q (x_k - x_r) +$ 
       $\sum_{k=0}^{L-1} a_k^T R a_k$ 
    subject to  $x_{k+1} = G^a x_k + H^a a_k$ 
       $x_{\min} \leq x_k \leq x_{\max}$ 
       $a_{\min} \leq a_k \leq a_{\max}$ 
     $s', r \leftarrow \text{step}(a_0)$   $\triangleright$  Take environment step
     $d \leftarrow d \oplus (s, a_0, r, s')$   $\triangleright$  add to trajectory
     $s \leftarrow s'$ 
  end for
  return  $s, d$   $\triangleright$  reached state, trajectory
end function

```

Table 2: Description of the 1D double-integrator test environment: a point mass M can be moved in a one-dimensional space $X = (\text{position}, \text{velocity})$ by applying a continuous-valued force. Reward is received based on the distance to two possible goal locations (G_1, G_2).

| | | |
|--|--|---------------------------|
| Dynamics | | |
| $X = \begin{bmatrix} x \\ \dot{x} \end{bmatrix}$ | $\dot{x} = Ax + Bu$ | |
| $A = \begin{bmatrix} 0 & 1 \\ 0 & 0 \end{bmatrix}$ | $B = \begin{bmatrix} 0 \\ 1 \end{bmatrix}$ | |
| Reward | | |
| $\max((1 - \tanh X - G_1^*), 2(1 - \tanh X - G_2^*))$ $G_1 = \begin{bmatrix} -2.5 \\ 0.0 \end{bmatrix}$ $G_2 = \begin{bmatrix} 6.0 \\ 0.0 \end{bmatrix}$ | | |
| Limits | | |
| $u \in [-1; 1]$ | $x \in [-10; 10]$ | $\dot{x} \in [-2.5; 2.5]$ |

future work.

7 Appendix

The approach implemented to calculate the AQR distance and to find the nearest state to a goal state x_r is summarized in Algorithm 3. The steering approach based on a linear MPC with shrinking horizon is summarized in Algorithm 4.

References

- Bradbury, J.; Frostig, R.; Hawkins, P.; Johnson, M. J.; Leary, C.; Maclaurin, D.; and Wanderman-Milne, S. 2018. JAX: Composable Transformations of Python+NumPy Programs. URL <http://github.com/google/jax>.
- Brockman, G.; Cheung, V.; Pettersson, L.; Schneider, J.; Schulman, J.; Tang, J.; and Zaremba, W. 2016. OpenAI Gym. *arXiv:1606.01540 [cs]* URL <http://arxiv.org/abs/1606.01540>.
- Camacho, E. F.; and Alba, C. B. 2007. *Model Predictive Control*. Springer Science & Business Media.
- Chatzilygeroudis, K.; Vassiliades, V.; Stulp, F.; Calinon, S.; and Mouret, J. 2020. A Survey on Policy Search Algorithms for Learning Robot Controllers in a Handful of Trials. *IEEE Transactions on Robotics* 36(2): 328–347.
- Dhariwal, P.; Hesse, C.; Klimov, O.; Nichol, A.; Plappert, M.; Radford, A.; Schulman, J.; Sidor, S.; Wu, Y.; and Zhokhov, P. 2017. OpenAI Baselines. *GitHub repository* URL <https://github.com/openai/baselines>.
- Ernst, D.; Geurts, P.; and Wehenkel, L. 2005. Tree-Based Batch Mode Reinforcement Learning. *Journal of Machine Learning Research* 6(Apr): 503–556.
- Glassman, E.; and Tedrake, R. 2010. A Quadratic Regulator-Based Heuristic for Rapidly Exploring State Space. In *2010 IEEE Int. Conf. Robotics and Automation (ICRA)*. IEEE.
- Haarnoja, T.; Zhou, A.; Hartikainen, K.; Tucker, G.; Ha, S.; Tan, J.; Kumar, V.; Zhu, H.; Gupta, A.; Abbeel, P.; and Levine, S. 2019. Soft Actor-Critic Algorithms and Applications. *arXiv:1812.05905 [cs, stat]* URL <http://arxiv.org/abs/1812.05905>.
- Henderson, P.; Islam, R.; Bachman, P.; Pineau, J.; Precup, D.; and Meger, D. 2018. Deep Reinforcement Learning That Matters. In McIlraith, S. A.; and Weinberger, K. Q., eds., *Proceedings of the Thirty-Second AAAI Conference on Artificial Intelligence, (AAAI-18), the 30th Innovative Applications of Artificial Intelligence (IAAI-18), and the 8th AAAI Symposium on Educational Advances in Artificial Intelligence (EAAI-18), New Orleans, Louisiana, USA, February 2-7, 2018*, 3207–3214. AAAI Press. URL <https://www.aaai.org/ocs/index.php/AAAI/AAAI18/paper/view/16669>.
- Hill, A.; Raffin, A.; Ernestus, M.; Gleave, A.; Traore, R.; Dhariwal, P.; Hesse, C.; Klimov, O.; Nichol, A.; Plappert, M.; Radford, A.; Schulman, J.; Sidor, S.; and Wu, Y. 2018. Stable Baselines. *GitHub repository* URL <https://github.com/hill-a/stable-baselines>.
- Hollenstein, J. J.; and Piater, J. 2019. Evaluating Planning for Policy Search. In *1st Workshop on Workshop on Closing the Reality Gap in Sim2real Transfer for Robotic Manipulation*. URL <https://sim2real.github.io/assets/papers/hollenstein.pdf>.
- Hollenstein, J. J.; Renaudo, E.; Matteo, S.; and Piater, J. 2020. How Does Explicit Exploration Influence Deep Reinforcement Learning? In *Joint Austrian Computer Vision and Robotics Workshop*, 29–30. Verlag der TU Graz. doi: 10.3217/978-3-85125-752-6.
- Hollenstein, J. J.; Renaudo, E.; and Piater, J. 2019. Improving Exploration of Deep Reinforcement Learning Using Planning for Policy Search. URL <https://openreview.net/forum?id=rJe7CkrFvS>.
- James, S.; Davison, A. J.; and Johns, E. 2017. Transferring End-to-End Visuomotor Control from Simulation to Real World for a Multi-Stage Task. *CoRR* abs/1707.02267. URL <http://arxiv.org/abs/1707.02267>.
- Karaman, S.; and Frazzoli, E. 2011. Sampling-Based Algorithms for Optimal Motion Planning. *The international journal of robotics research* 30(7): 846–894.
- Lange, S.; Gabel, T.; and Riedmiller, M. 2012. Batch Reinforcement Learning. In *Reinforcement Learning*, 45–73. Springer.
- Lavalle, S. M. 1998. Rapidly-Exploring Random Trees: A New Tool for Path Planning. Technical report.
- Levine, S.; and Koltun, V. 2013. Guided Policy Search. In *Proceedings of the 30th International Conference on Machine Learning (ICML-13)*, 1–9. URL <http://www.jmlr.org/proceedings/papers/v28/levine13.pdf>.
- Lillicrap, T. P.; Hunt, J. J.; Pritzel, A.; Heess, N.; Erez, T.; Tassa, Y.; Silver, D.; and Wierstra, D. 2016. Continuous Control with Deep Reinforcement Learning. In *Proc. 4th Int. Conf. Learning Representations, (ICLR)*. URL <http://arxiv.org/abs/1509.02971>.
- Mandlekar, A.; Zhu, Y.; Garg, A.; Fei-Fei, L.; and Savarese, S. 2017. Adversarially Robust Policy Learning: Active Construction of Physically-Plausible Perturbations. In *2017 IEEE/RSJ International Conference on Intelligent Robots and Systems (IROS)*, 3932–3939. doi:10.1109/IROS.2017.8206245.
- Moore, A. W. 1990. Efficient Memory-Based Learning for Robot Control .
- Muratore, F.; Treede, F.; Gienger, M.; and Peters, J. 2018. Domain Randomization for Simulation-Based Policy Optimization with Transferability Assessment. In *Conference on Robot Learning*, 700–713.
- Murray, R.; Murray, R. M.; and Hauser, J. 1990. A Case Study in Approximate Linearization: The Acrobot Example .
- OpenAI; Andrychowicz, M.; Baker, B.; Chociej, M.; Józefowicz, R.; McGrew, B.; Pachocki, J.; Petron, A.; Plappert, M.; Powell, G.; Ray, A.; Schneider, J.; Sidor, S.; Tobin, J.; Welinder, P.; Weng, L.; and Zaremba, W. 2018. Learning Dexterous In-Hand Manipulation. *CoRR* URL <http://arxiv.org/abs/1808.00177>.

- Perez, A.; Platt, R.; Konidaris, G.; Kaelbling, L.; and Lozano-Perez, T. 2012. LQR-RRT*: Optimal Sampling-Based Motion Planning with Automatically Derived Extension Heuristics. In *IEEE Int. Conf. Robotics and Automation*. doi:10.1109/ICRA.2012.6225177.
- Plappert, M.; Houthoofd, R.; Dhariwal, P.; Sidor, S.; Chen, R. Y.; Chen, X.; Asfour, T.; Abbeel, P.; and Andrychowicz, M. 2017. Parameter Space Noise for Exploration. *CoRR* abs/1706.01905. URL <http://arxiv.org/abs/1706.01905>.
- Renaudo, E.; Girard, B.; Chatila, R.; and Khamassi, M. 2014. Design of a Control Architecture for Habit Learning in Robots. In *Biomimetic and Biohybrid Systems, LNAI Proceedings*, 249–260. doi:10.1007/978-3-319-09435-9_22. URL http://dx.doi.org/10.1007/978-3-319-09435-9_22.
- Sadeghi, F.; and Levine, S. 2017. CAD2RL: Real Single-Image Flight Without a Single Real Image. In *Robotics: Science and Systems*.
- Saveriano, M.; Yin, Y.; Falco, P.; and Lee, D. 2017. Data-Efficient Control Policy Search using Residual Dynamics Learning. In *International Conference on Intelligent Robots and Systems*, 4709–4715.
- Schulman, J.; Levine, S.; Moritz, P.; Jordan, M.; and Abbeel, P. 2015. Trust Region Policy Optimization. In *Proceedings of the 32Nd International Conference on International Conference on Machine Learning - Volume 37, ICML'15*, 1889–1897. Lille, France: JMLR.org. URL <http://dl.acm.org/citation.cfm?id=3045118.3045319>.
- Schulman, J.; Wolski, F.; Dhariwal, P.; Radford, A.; and Klimov, O. 2017. Proximal Policy Optimization Algorithms. *CoRR* abs/1707.06347.
- Silver, D.; Huang, A.; Maddison, C. J.; Guez, A.; Sifre, L.; van den Driessche, G.; Schrittwieser, J.; Antonoglou, I.; Panneershelvam, V.; Lanctot, M.; Dieleman, S.; Grewe, D.; Nham, J.; Kalchbrenner, N.; Sutskever, I.; Lillicrap, T.; Leach, M.; Kavukcuoglu, K.; Graepel, T.; and Hassabis, D. 2016. Mastering the Game of Go with Deep Neural Networks and Tree Search. *Nature* 529(7587): 484–489. ISSN 1476-4687. doi:10.1038/nature16961.
- Sutton, R. S.; and Barto, A. G. 2018. *Reinforcement Learning: An Introduction*. The MIT Press, second edition. URL <http://incompleteideas.net/book/the-book-2nd.html>.
- Tassa, Y.; Erez, T.; and Todorov, E. 2012. Synthesis and Stabilization of Complex Behaviors through Online Trajectory Optimization. In *Intelligent Robots and Systems (IROS), 2012 IEEE/RSJ International Conference On*, 4906–4913. IEEE.
- Tobin, J.; Fong, R.; Ray, A.; Schneider, J.; Zaremba, W.; and Abbeel, P. 2017. Domain Randomization for Transferring Deep Neural Networks from Simulation to the Real World. In *Intelligent Robots and Systems (IROS), 2017 IEEE/RSJ International Conference On*, 23–30. IEEE.
- Todorov, E.; and Weiwei Li. 2005. A Generalized Iterative LQG Method for Locally-Optimal Feedback Control of Constrained Nonlinear Stochastic Systems. In *Proceedings of the 2005, American Control Conference, 2005.*, 300–306. Portland, OR, USA: IEEE. ISBN 978-0-7803-9098-0. doi:10.1109/ACC.2005.1469949.
- Wolfslog, W. J.; Bharatheesha, M.; Moerland, T. M.; and Wisse, M. 2018. RRT-CoLearn: Towards Kinodynamic Planning Without Numerical Trajectory Optimization. *IEEE Robotics and Automation Letters* 3(3): 1655–1662. ISSN 2377-3766. doi:10.1109/LRA.2018.2801470.
- Žlajpah, L. 1998. Simulation of Nr Planar Manipulators. *Simulation Practice and Theory* 6(3): 305–321.